

Third International Conference on Multidisciplinary
Design Optimization and Applications,
June 21-23, 2010 Paris, France
www.asmdo.com/conference2010/

Detection on debondings in FRP-strengthened reinforced concrete beams

R. Perera*, A. Ruiz^a

^(*)*Department of Structural Mechanics, Technical University of Madrid,
José Gutiérrez Abascal 2, 28006 Madrid, Spain
perera@etsii.upm.es*

^(a)*Department of Applied Mathematics, Technical University of Madrid,
Alenza 4, 28003 Madrid, Spain
antonio.ruizp@upm.es*

Abstract

Advanced composite materials are increasingly used in the strengthening of reinforced concrete (RC) structures. This strengthening method is often associated with a brittle and sudden failure caused by some form of FRP bond failure which may be originated at the termination of the FRP material and propagate towards the midspan or in the vicinity of flexural cracks in the RC beam and propagate towards the FRP termination. Hence, flexural cracking of the RC beam has a major influence on the overall response of the strengthened member, and it affects the distribution of the stresses in the various constituents of the strengthened member. In addition, this failure mode will affect the dynamic response of the beam by altering its natural frequencies. As a result, considerable analytical, numerical and experimental efforts should be made to capture these phenomena. An optimization method based on spectral elements is proposed here for detection of local debondings in RC beams externally strengthened with FRP.

1 Introduction

Advanced composite materials are increasingly used in the strengthening of reinforced concrete (RC) structures (Bank [1]). The use of externally bonded strips made of fibre-reinforced plastics (FRP) as strengthening method has gained widespread acceptance in recent years since it has many advantages over the traditional techniques, especially because of the high strength and modulus of elasticity, improved durability, and low weight of the composite material. Failure of FRP-strengthened RC beams may take a variety of forms including all those associated with conventional concrete beams. However, unfortunately, this strengthening method is often associated with a brittle and sudden failure caused by some form of FRP bond failure. This kind of failure is produced in the form of cover delamination, i.e., along the plane of the steel reinforcement, or FRP delamination, i.e., in the plane along the FRP-concrete interface. Furthermore, failure may be originated at the termination of the FRP material and propagate towards the midspan (Yang et al. [7], Pesic et al. [4]) or in the vicinity of flexural cracks in the RC beam and propagate towards the FRP termination (Sebastian [6], Yao et al. [8]). Hence, flexural cracking of the RC beam has a major influence on the overall response of the strengthened member, and it affects the distribution of the stresses in the various constituents of the strengthened member.

The topic of structural health monitoring has been scarcely developed in FRP strengthened RC beams in spite of its importance to prevent brittle failure modes. This work proposes a first approach to develop this topic which should be extended increasingly in the future. For it, a spectral finite element (SFE) model (Doyle [2]) is implemented in the framework of FRP-strengthened RC beams.

2 Differential equations

Considering first-order shear deformation theory, the axial and transverse displacement field can be expressed as:

$$u_C(x, z, t) = u_0(x, t) - z\phi(x, t) \quad (1)$$

$$u_{FRP}(x, z, t) = u_0(x, t) - z\phi(x, t) + s(x, t) \quad (2)$$

$$w(x, z, t) = w(x, t) \quad (3)$$

where u_C , u_{FRP} and w are respectively the axial displacements in RC beam and FRP plate and the transverse displacement at a material point, ϕ is the curvature-independent rotation of the beam cross-section about the Y-axis and s is the interface slip.

The linear constitutive model for the concrete beam and the FRP plate can be expressed as

$$\sigma_{xC} = E_C \varepsilon_{xC} \quad \tau_{xzC} = G_C \gamma_{xzC} \quad (4)$$

$$\tau_{xzFRP} = G_{FRP} \gamma_{xzFRP} \quad (5)$$

where the material constants, E and G , are referred to the concrete beam (C) or the external plate (FRP) depending on the material considered.

Applying Hamilton's principle, the governing equations of the FRP flexural strengthened RC beam are obtained and can be written as

$$\delta u_0 : I_0 \ddot{u}_0 - I_1 \ddot{\phi} + I_{0FRP} \ddot{s} - A_{11} u_{0,xx} + B_{11} \phi_{,xx} - A_{FRP} s_{,xx} = 0 \quad (6)$$

$$\delta w : I_0 \ddot{w} - A_{22} w_{,xx} + A_{22} \phi_{,x} = 0 \quad (7)$$

$$\delta \phi : I_2 \ddot{\phi} - I_1 \ddot{u}_0 - I_{1FRP} \ddot{s} + B_{11} u_{0,xx} - D_{11} \phi_{,xx} - A_{22} w_{,x} + A_{22} \phi + B_{FRP} s_{,xx} = 0 \quad (8)$$

$$\delta s : I_{0FRP} \ddot{s} + I_{0FRP} \ddot{u}_0 - I_{1FRP} \ddot{\phi} - A_{FRP} s_{,xx} - A_{FRP} u_{0,xx} + B_{FRP} \phi_{,xx} + \frac{G_{AD} s b_{AD}}{e_{AD}} = 0 \quad (9)$$

and associated force boundary equations can be expressed as

$$N = A_{11} u_{0,x} - B_{11} \phi_{,x} + A_{FRP} s_{,x} \quad (10)$$

$$V = A_{22} w_{,x} - A_{22} \phi \quad (11)$$

$$M = -B_{11} u_{0,x} + D_{11} \phi_{,x} - B_{FRP} s_{,x} \quad (12)$$

$$N^* = A_{FRP} s_{,x} + A_{FRP} u_{0,x} - B_{FRP} \phi_{,x} \quad (13)$$

where (\cdot) denotes temporal derivative. N , V , M and N^* are the stress resultants associated with the variables u_0 , w , ϕ and s , respectively.

A_{11} , B_{11} , D_{11} , A_{22} , A_{FRP} and B_{FRP} are the stiffness coefficients obtained from the material properties:

$$[A_{11} \ B_{11} \ D_{11}] = \int_{z_{C1}}^{z_{C2}} E_C [1 \ z \ z^2] b_C dz + \int_{z_{FRP1}}^{z_{FRP2}} E_{FRP} [1 \ z \ z^2] b_{FRP} dz + \sum_{j=1}^{NSS} E_{sj} A_{sj} [1 \ z_j \ z_j^2] \quad (14)$$

$$[A_{22}] = \int_{z_{C1}}^{z_{C2}} G_C b_C dz + \int_{z_{FRP1}}^{z_{FRP2}} G_{FRP} b_{FRP} dz \quad (15)$$

$$[A_{FRP} \ B_{FRP}] = \int_{z_{FRP1}}^{z_{FRP2}} E_{FRP} [1 \ z] b_{FRP} dz \quad (16)$$

3 Formulation of spectral elements

A spectral Timoshenko beam finite element formulation for the problem under consideration has been considered (Gopalakrishnan et al.[3]). The generic displacement vector at any point and frequency becomes

$$\begin{Bmatrix} \hat{u}_0(x, \omega_n) \\ \hat{w}(x, \omega_n) \\ \hat{\phi}(x, \omega_n) \\ \hat{s}(x, \omega_n) \end{Bmatrix} = \begin{bmatrix} R_{11} & \dots & R_{18} \\ R_{21} & \dots & R_{28} \\ R_{31} & \dots & R_{38} \\ R_{41} & \dots & R_{48} \end{bmatrix} \begin{bmatrix} e^{-jk_1x} & 0 & \dots & 0 \\ 0 & e^{-jk_2x} & \dots & 0 \\ \vdots & \ddots & \ddots & \vdots \\ 0 & \dots & \dots & e^{-jk_8x} \end{bmatrix} \{A(\omega_n)\} \quad (17)$$

where $k_{p+4} = -k_p$ ($p=1, \dots, 4$) are the wavenumbers.

$\{A\}_n$ is a vector of eight unknown constants to be determined. This vector can be calculated by imposing the nodal spectral displacements at the two nodes of the element.

The dynamic stiffness matrix is formulated by using the force boundary conditions at the nodes of the element.

4 Numerical results

To evaluate how the presented numerical model is able to simulate the nonlinear static behaviour of the FRP-strengthened beams, results from one experimentally tested beam taken from the literature have been used first.

The experimental case deals with the response of the B8 rectangular RC beam strengthened by externally bonded glass FRP strip, which was tested in Rahimi and Hutchinson [5]. The beam was 2.3 m long x 0.2 m wide x 0.15 m deep (Figure 1) and was reinforced longitudinally with two bars of 0.008 m diameter over compression side and two bars of 0.010 m diameter over tension side; transversally, stirrups of 0.006 m diameter at every 0.075 m were distributed along the beam. The glass FRP plate used with the B8 specimen was 1.930 m long and 0.15 m wide and its thickness was 0.0018 m. The beam was subjected to two identical point loads, applied symmetrically at 0.3 m from the middle (four-point bending test), being simply supported on a pivot bearing on one side and a roller bearing on the other side, over a span of 2.1 m; 43 spectral finite elements were used, one for each one of the two non-strengthened beam portions in the vicinity of the supports, another one for the beam portion between the applied loads and 20 elements uniformly distributed at the beam portions located between the ends of the FRP plate and the loads. The properties of materials used are shown in Table 1. The compressive strength for concrete is defined between 54 and 69 MPa in the table. After some numerical tests, the maximum value (69 MPa) was chosen in all the calculations. The plastic hardening coefficient for the steel reinforcement was assumed to be 1% of Young's modulus. A bilinear behaviour law was assumed for the adhesive determined from the adhesive properties in Table 1.

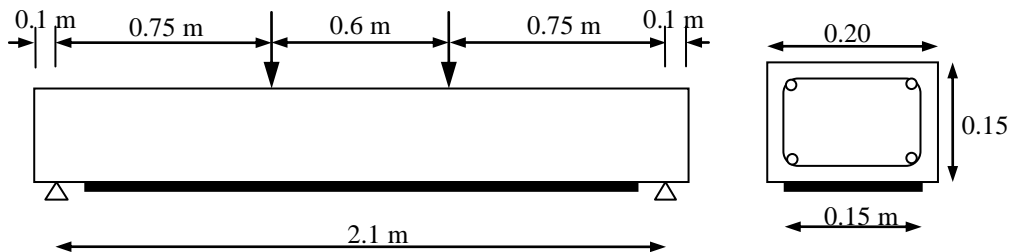


Figure 1: Details of the geometry of the B8 RC beam

Table 1. Properties of materials used in B8 beam

Property	Concrete	GFRP	CFRP	Adhesive	Internal steel reinforcement
Density(Kg/m ³)	2000	2200	1500	1500	7800
Young's modulus(GN/m ²)	25	36	127	7	210
Shear strength(MN/m ²)	6	-	80	27	-
Tensile strength(MN/m ²)	3	1074	1532	25	575
Compressive strength(MN/m ²)	54-69	-	-	70	-
Fracture energy(KJ/m ²)	0.02	-	-	0.4	-
Poisson's ratio	0.2	0.3	0.3	0.3	0.3
Elongation at break(%)	0.15	3.1	1.21	0.7	>20

Figure 2 shows the comparison of the spectral model prediction of the load-deflection response of the strengthened beam B8, along with the experimental results. As in the previous example, the results show a reasonable accuracy in predicting the load-displacement behaviour, especially considering the uncertainty regarding concrete material behaviour.

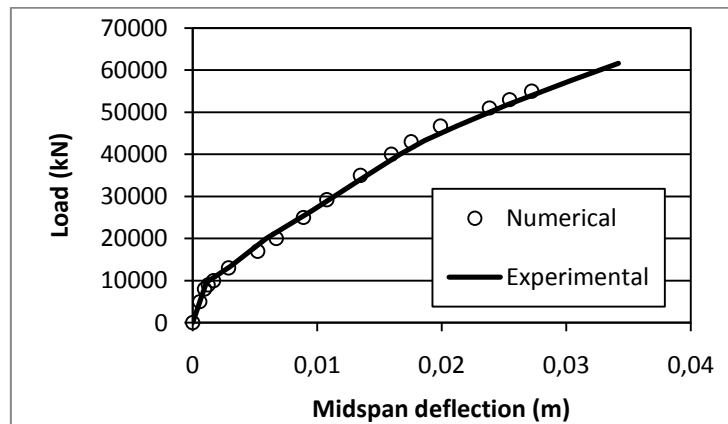


Figure 2: Load-deflection behaviour

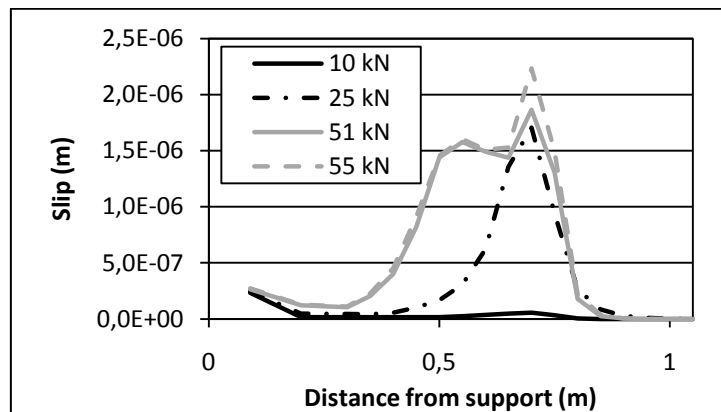


Figure 3: Interface slip evolution

The local behaviour at the adhesive-concrete interface considering flexural cracking of the RC beam is shown in Figure 3 by using the interface-slip evolution under increasing load levels. In the same way, the evolution of the axial stress in steel rebars and FRP plate are shown in Figures 4 and 5. According to the experimental results the beam failed as a result of transverse curling of the plate at the midspan. In Figure 3, the maximum peak value of the interface slip is located where there is steel rebar yielding, since, in that case, a sudden increase in FRP strain rate occurs starting from that region. Results demonstrates the ability of the proposed method to simulate intermediate debonding failure and, therefore, to be used in an interface damage identification procedure.

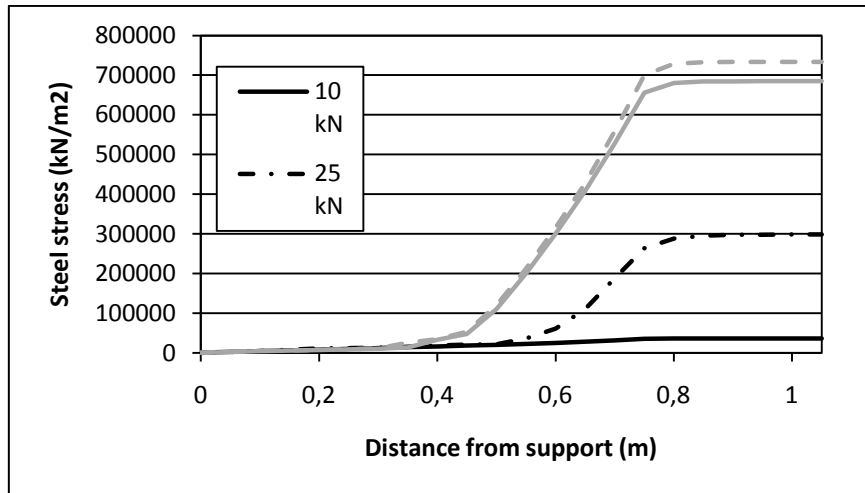


Figure 4: Evolution of the predicted stress in the tensile steel rebar

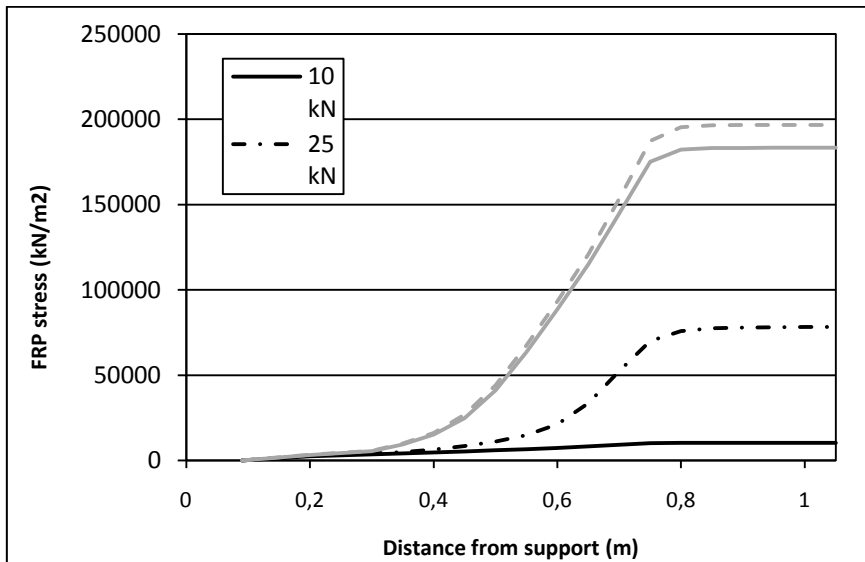


Figure 5: Evolution of the predicted stress in the FRP plate

5 Damage identification

The model derived previously can be used to develop numerical algorithms for damage detection studies. Damage identification is essentially an inverse problem which requires the application of model updating techniques and the formulation of suitable objective functions. Performance of the procedure largely depends upon the objective function. Different objective functions based on static parameters are examined from a numerical point of view. Genetic algorithms (GAs) are used to solve the inverse problem. Genetic algorithms are powerful and widely applicable stochastic search and optimization algorithms based on the principle of natural selection and genetic evolution. The main advantage of GAs lies in their robustness in handling non-smooth problems. Results will be presented.

6 Conclusions

A model using spectral elements has been proposed to simulate in a unified way the static and dynamic behaviour of FRP flexural strengthened reinforced concrete beams. The two main characteristics of the proposed approach are its simplicity and its ability in accurate high-frequency modelling. This model can be taken as a starting point to implement a damage identification procedure for this kind of strengthening.

Acknowledgements

The writers acknowledge the support for the work reported in this paper from the Spanish Ministry of Education and Science (project BIA2007-67790).

References

- [1] Bank, LC. In *Composites for construction: Structural design with FRP materials*, first ed. John Wiley and Sons, 2006.
- [2] Doyle, JF, In *Wave Propagation in Structures*, first ed. Springer, New York, 1997.
- [3] Gopalakrishnan, S, Ghakraborty, A, Roy Mahapatra, D. In *Spectral finite element method*, first ed. Springer, London 2008.
- [4] Pestic, N, Pilakoutas, K. Concrete beams with externally bonded flexural FRP-reinforcement: analytical investigation of debonding failure, In *Compos. Part B-: Eng*, 2003; 34(4), 327-338.
- [5] Rahimi, A, Hutchinson, A. Concrete Beams Strengthened with Externally Bonded FRP Plates, In *J. Compos. Constr*, 2001, 5(1), 44-56.
- [6] Sebastian, WM. Significance of midspan debonding failure in FRP-plated concrete beams, In *J. Struct. Eng. ASCE* 2001, 127(7), 792-798.
- [7] Yang, ZJ, Chen, JF, Proverbs, D. Finite element modelling of concrete cover separation failure in FRP plated RC beams, In *Constr. Build. Mater*, 2003, 17 (1), 3-13.
- [8] Yao, J, Teng, JG, Lam, L. Experimental study on intermediate crack debonding in FRP-strengthened RC flexural members, In *Adv. Struct. Eng* 2005, 8 (4), 365-396.